Akbiyik *et al.*
Journal of Analytical Science and Technology (2025) 16:23
https://doi.org/10.1186/s40543-025-00495-z

Journal of Analytical Science and Technology

RESEARCH ARTICLE **Open Access**

The usage of $TiO_2@Fe_3O_4$ nanocomposites synthesized by a novel and facile method as adsorbents in the separation/preconcentration of silver ions from domestic wastewater samples

Hilal Akbiyik[1], Ayça Girgin[1,2], Buse Tuğba Zaman[1], Arda Atakol[3,4,5], Nevim San[1] and Sezgin Bakirdere[1,6*]

Abstract

Global population growth has led to an increase in the consumption of silver, which has a wide range of applications. This situation has increased demand for determining trace levels of silver to protect public health and the environment. In this study, an efficient magnetic-dispersive solid phase extraction (MDSPE) method was developed utilizing $TiO_2@Fe_3O_4$ nanocomposites (NCs) as adsorbent for the separation and preconcentration of silver ions. TiO_2 nanoparticles (NPs) were synthesized by a microwave-assisted hydrothermal method under different precursor solution and temperature program conditions. The procedure yielding TiO_2 NPs with the homogeneous size distribution was established, and the NPs obtained with this procedure were used to modify the Fe_3O_4 surface. $TiO_2@Fe_3O_4$ NCs and TiO_2 NPs synthesized via alternative innovative methods to traditional techniques were examined by various characterization methods. Flame atomic absorption spectrometry (FAAS) was used for detection and quantification of analyte. All parameters expected to affect the adsorption and desorption of silver ions on the $TiO_2@Fe_3O_4$ NCs were optimized. In the developed procedure, the optimum parameters were 20 mg $TiO_2@Fe_3O_4$ NC, 1.5 mL potassium hydrogen phthalate buffer solution (pH 6.0), orbital agitation for 30 min, and 0.10 mL HNO_3 (2.0 M). The proposed novel $TiO_2@Fe_3O_4$-MDSPE-FAAS method exhibits detection and quantification limits of 0.005 and 0.017 mg kg^{-1} in a wide linear working range for silver ions. The method's relevance and accuracy were evaluated by recovery experiments conducted on both actual and synthetic residential wastewater samples, yielding satisfactory percent recovery results using a matrix-matching calibration strategy.

Keywords Titanium dioxide, $TiO_2@Fe_3O_4$, Dispersive solid phase extraction, Silver ions, Wastewater

---

*Correspondence:
Sezgin Bakirdere
bsezgin@yildiz.edu.tr
Full list of author information is available at the end of the article

Graphical abstract

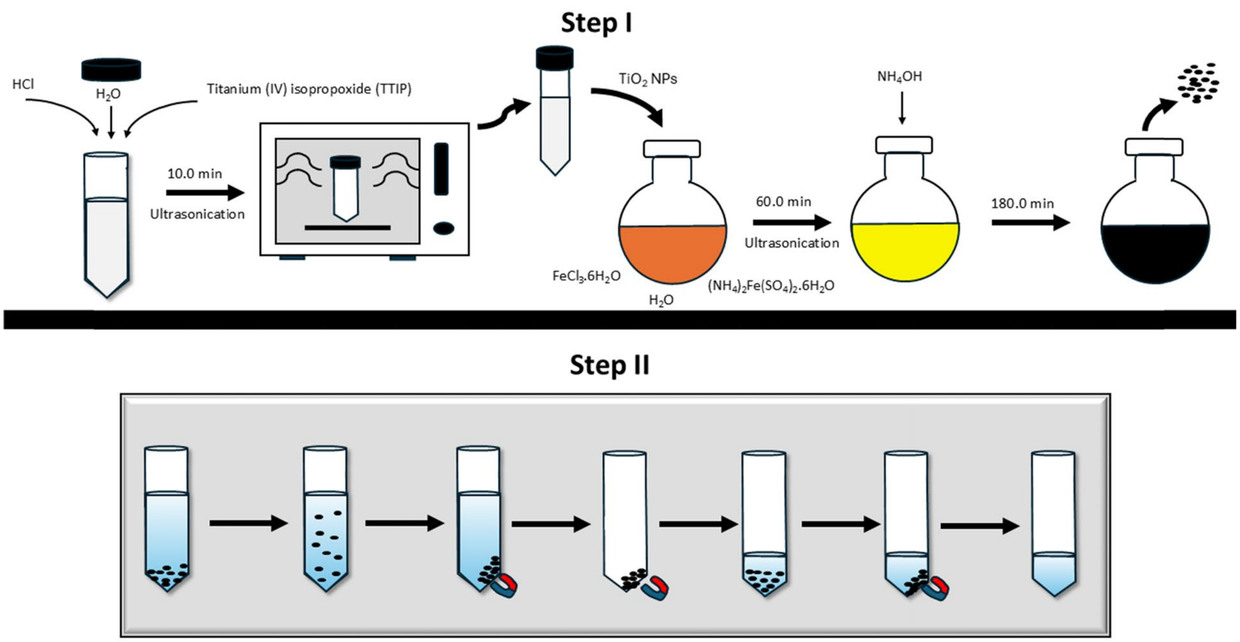

Introduction

Industrialization advancement and global population expansion have not only intensified the demand for natural reserves and energy resources but also increased the generation of industrial and domestic wastewater (Nguyen and Wu 2024). The considerable amount of domestic wastewater produced each day is recognized as a crucial environmental concern in the twenty-first century, threatening water security, ecosystem integrity, and overall public health (Seetasang and Iwai 2025). These wastewaters are abundant in suspended matter, organic pollutants, and heavy metals exhibiting elevated biological oxygen demand (BOD5) and chemical oxygen demand (COD) values (El Hafidi et al. 2023). Heavy metals are incorporated into domestic wastewater through water used in cooking, laundering, toilet flushing, and bathing (van den Brand et al. 2015). The most common heavy metals contained in this matrix are silver (Ag), cadmium (Cd), manganese (Mn), lead (Pb), zinc (Zn), iron (Fe), chromium (Cr), nickel (Ni), mercury (Hg), and copper (Cu) (Muoghalu et al. 2023). Ag is known to be toxic and vital to various biological systems and has been continuously released into the environment through wastewater discharge in the last decade (Al-Saidi and Khan 2024; Naeemullah et al. 2016). It is employed in antiviral, bactericidal, anti-inflammatory, antibacterial and therapeutic applications, instrument disinfection, burn care, and wound healing (Ouyang et al. 2024; Tang et al. 2024; Xu et al. 2020). Despite its advantages, exposure to elevated concentrations of silver in several forms has been documented to be highly toxic to the majority of aquatic organisms, including fish (Choi and Cui 2012). Furthermore, Ag has some detrimental effects on human health; for example, ingestion or prolonged exposure can lead to health problems such as gastric disorders, argyria, legionella pneumophila, skin allergies, kidney diseases, and organ edema (Huang et al. 2017; Kaur et al. 2023).

Ag ions which are soluble in water systems have been classified as hazardous substances by the US Environmental Protection Agency (EPA) and the World Health Organization (WHO) (Song et al. 2011). The maximum concentration of Ag^+ for safe drinking water set by EPA is 0.05 mg L^{-1} (or 0.465 µmol L^{-1}), while WHO recommends 0.1 mg L^{-1} (or 0.93 µmol L^{-1}) (Wu et al. 2023). Therefore, it is required to develop highly sensitive, rapid, and selective analytical strategies for the detection of silver ions at trace levels to monitor water quality and to protect the environment and human health (Gao et al. 2017; Ji et al. 2018).

Analytical instrumental systems such as UV–Vis spectrophotometry (Zengin and Gürkan 2021), inductively coupled plasma–mass spectrometry (ICP-MS) (Chronakis et al. 2023), flame atomic absorption spectrometry (FAAS) (Roushani et al. 2016), ICP optical emission spectrometry (ICP-OES) (Gasbarri et al. 2019), fluorescence spectrometry (Liu et al. 2022) were used for Ag determination. Sample preparation procedures for the accurate determination of target analytes in various matrices remain relevant even with all the significant advances in analytical instrumentation (Sajid and Płotka-Wasylka 2018). One of the reasons for this is the growing popularity of samples containing complex matrices, especially in modern analytical chemistry applications (Xia et al. 2020). The solid phase microextraction (SPME) technique has been recognized by many scientists as it has superior features such as rapid analysis, low sample volume, and opportunities for automation (Płotka-Wasylka et al. 2015). Due to its outstanding properties and enormous potential in analytical applications, many studies have been conducted to improve the efficiency and sensitivity of the SPME technology and to develop novel approaches for integration with various instrumentations (Spietelun et al. 2013). To overcome the limitations in traditional SPME such as long extraction durations, relatively poor reproducibility, and low service life associated with commercially available materials, the focus in recent years has been on synthesizing novel sorbents (Khezeli and Daneshfar 2017). At this point, nanomaterials have been considered as attractive materials for SPME techniques since they have the potential to increase extraction efficiency due to their properties such as high surface area, large adsorption capacity, high porosity, and fast sorption kinetics (Jagirani and Soylak 2020). Metallic nanoparticles, carbonaceous nanomaterials, silicon-based nanomaterials, carbon nanotubes, metal oxide nanoparticles, and magnetic nanoparticles are some of the nanomaterials used in sample preparation procedures (Ahmadi et al. 2017). The metal oxide nanoparticles stand out with their high adsorption capacity and specific surface area as well as high chemical, thermal, and mechanical stability (Pyrzynska 2020). TiO_2 is widely used due to its favorable properties such as being low cost, stable for a long time, non-toxic, and relatively easy to synthesize (Yalcin 2022). The strong polarity of the Ti–O bond in its structure polarizes the water molecules adsorbed on its surface and forms hydrophilicity-enhanced hydroxyl groups, creating a high performing adsorbent (Liu et al. 2023). Nevertheless, its use individually in nanoscale extraction studies is rare (Gutiérrez-Fernández et al. 2024). Unless they are functionalized or modified, titanium dioxide nanoparticles tend to disperse in aqueous solutions in a way that makes it difficult to separate them from the solution because of their tiny size (Habila et al. 2016). Fe_3O_4 nanoparticles have been known to facilitate nanosorbent isolation from solution thanks to their magnetic properties (Aladaghlo et al. 2024). Hence, Fe_3O_4 and TiO_2 particles can be combined to benefit from this advantage (Al-Salihi et al. 2022).

In this study, TiO_2 NPs were synthesized by a simple and effective method and transformed into nanocomposites by combining with Fe_3O_4 nanoparticles. The potential of the obtained nanocomposites as an efficient adsorbent for the separation/preconcentration of Ag ions was assessed in domestic wastewater samples. To the best of our knowledge, $TiO_2@Fe_3O_4$ NCs has not been used as adsorbent for silver ion in the literature.

Experimental

Apparatus

A Smart D model microwave digestion system purchased from Milestone was used to synthesize TiO_2 nanomaterials. A Malvern PANalytical (UK) X'Pert Pro X-Ray diffractometer (XRD), a Malvern PANalytical (UK) Nano ZS zeta potential analyzer, a Thermo Fischer Scientific (USA) Apreo 2S LoVac Schottky field emission scanning electron microscope (FE-SEM), and a Zeiss (Germany) EVO LS 10 scanning electron microscope (SEM) were used for the characterization of the TiO_2 and $TiO_2@Fe_3O_4$ nanomaterials. XRD measurements were taken in the range of 10–90° 2θ in continuous scanning mode at room temperature with copper as the anode material, 40 mA tube current, 45 kV accelerating voltage. A Unicam (UK) Solaar 929 AA series flame atomic absorption spectrometer was utilized for the absorbance measurements. A multi-element hollow cathode lamp (Photron, Australia), which provides the characteristic emission radiation of silver, lead and cadmium metals, and a D_2 lamp for the background correction were utilized. Acetylene–air fuel–oxidant mixture was preferred for the stoichiometric flame of the system. An analytical balance (SHIMADZU ATX-224R, Japan), an orbital stirrer (Biobase, China), a pH meter (Mettler Toledo, USA), a vortex mixer (Isolab, Germany), a centrifuge (Biobase, China), an ultrasonic bath (Runyes Medikal, China), a ventilated oven (Heraeus, Germany), and a heated magnetic stirrer (IKA, Germany) were used during the experimental studies.

Chemicals and reagents

In the synthesis of TiO_2 NPs, titanium (IV) isopropoxide (TTIP) (Sigma-Aldrich, Germany, 97%) and hydrochloric acid (HCl) (Merck, Germany, 37%) were employed as a titanium source and as a catalyst, respectively. For the synthesis of $TiO_2@Fe_3O_4$ NCs, ammonium iron (II) sulfate hexahydrate salt ($(NH_4)_2Fe(SO_4)_2.6H_2O$,) (Merck, Germany, ≥ 99%) and iron (III) chloride hexahydrate salt ($FeCl_3.6H_2O$) (Isolab, Germany, ≥ 97%) were used. A CertiPur grade Ag^+ stock standard solution (1000 ± 2 mg L^{-1}, $AgNO_3$ in 0.50 mol L^{-1} HNO_3) was purchased from Merck for use in experimental studies for silver determination. The same company supplied ethyl alcohol (EtOH, 99.9%), nitric acid (HNO_3, 65%), and ammonia (NH_4OH, %25) reagents. AMBERLITE IRA-96SB resin (ROHM AND HAAS, France) was utilized to remove anions in the sample preparation step. Potassium hydrogen phthalate (AmBeed, USA, 99.68%), tris-hydroxymethyl aminomethane (MilliporeSigma, Merck, Germany), and di-sodium tetraborate decahydrate (Merck, Germany, 99–103%) salts were preferred for the preparation of buffer solutions. The following chemicals were provided for the preparation of domestic wastewater: sodium bicarbonate (ChemBio, Türkiye), D- (+) glucose monohydrate (Sigma-Aldrich, Germany, 97.5–102.0%), potassium phosphate monobasic (Riedel–deHaen, Germany, 99.5–100.5%), and ammonium sulfate (Isolab, Germany, ≥ 99.5%). Manganese (II) sulfate monohydrate (99.0—101.0%), calcium chloride, and magnesium sulfate heptahydrate (99.0–100.5%) salts were supplied by Merck.

Synthesis of TiO_2 nanoparticles

Six different procedures have been employed for the synthesis of TiO_2 NPs. Accordingly, two different TiO_2 precursor solutions were prepared and three distinct temperature programs were tested used. The results are discussed in detail in the "3.1. Characterization studies" section. To prepare precursor solution-A, 1.4 mL of each TTIP, deionized water and HCl was taken and mixed in a centrifuge tube. In precursor solution-B, these volumes were tripled. White particles appeared when deionized water was added to TTIP in both precursor solutions. After mixing all constituents, the solutions were maintained under ultrasonication for 10.0 min. At the end of ultrasonication, the particles dissolved, and a homogeneous solution was obtained. Afterward, the precursor solution was transferred to a high-pressure and high-temperature resistant Teflon vessel. Following the transfer, the centrifuge tubes were washed with 5.8 mL and 2.4 mL of water for precursor solutions A and B, respectively, to minimize the loss of components. The Teflon vessel was then sealed to eliminate contact with air and placed in the microwave digestion system. In the three temperature programs performed, the temperature was first elevated from room temperature to 90 °C during the first 5.0 min and maintained at that level for an additional 5.0 min. All three programs are identical up to this stage. The temperature was elevated to 145, 150, or 155 °C based on the chosen program within 5.0 min starting from the 10th minute and maintained at this level for 15.0 min. Finally, the programs were completed by cooling for 10.0 min. The precursor solutions and temperature programs investigated in this study are summarized in Table 1. After evaluating the characterization results discussed in Sect. "Characterization studies", TiO_2 NPs prepared with precursor solution-A and program-3 were preferred in the synthesis of $TiO_2@Fe_3O_4$ NCs.

Synthesis of magnetic $TiO_2@Fe_3O_4$ nanocomposites

The TiO_2 colloidal nanoparticle mixture was exposed to ultrasound for 10.0 min before use. Meanwhile, 0.9805 g (2.5 mmol) $(NH_4)_2Fe(SO_4)_2.6H_2O$ and 1.3515 g (5.0 mmol) $FeCl_3.6H_2O$ salts were weighed and transferred to a reaction flask. The salts were dissolved by adding 95.0 mL of deionized water. 5.0 mL of TiO_2 colloidal nanoparticle mixture was added dropwise to the Fe(II)-Fe(III) solution in the reaction flask. The solution was subjected to ultrasonication for 60.0 min to ensure an effective dispersion. Upon completion of the specified

Table 1 Precursor solution and temperature program conditions investigated in TiO_2 NP synthesis

Precursor solution			Microwave digestion system temperature programs
Component	**A, mL**	**B, mL**	
TTIP	1.4	4.2	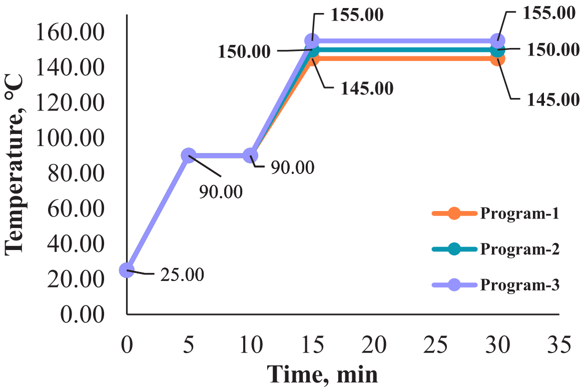
HCl	1.4	4.2	
Deionized water	7.2	6.6	
Final volume	10.0	15.0	

time, the reaction flask was removed from the ultrasonic bath and stirred in the heater with the aid of a magnetic stirrer. When the temperature reached 80 °C, 6.0 mL of NH_4OH was added dropwise to the mixture. The solution was kept in an inert atmosphere at 80 °C and stirred continuously for 3 h. The synthesized product was washed with deionized water and ethyl alcohol and dried in an oven operating at 50–55 °C for 24 h.

Extraction procedure

In the first step of the separation/preconcentration procedure, 20.0 mg of $TiO_2@Fe_3O_4$ NCs was weighed into a 15-mL centrifuge tube. Into the tube were added 8.0 mL of Ag aqueous standard or sample solution and 1.5 mL of potassium hydrogen phthalate-NaOH buffer solution adjusted to pH 6.0. It was then agitated in an orbital shaker for 30 min. After the agitation, the NCs were collected at the bottom of the tube by centrifugation. The analyte-rich adsorbent was readily separated from the solution by holding it with a neodymium magnet. Afterward, desorption was conducted by adding 0.10 mL of 2.0 M HNO_3 solution to the tube. The sample was vortexed for 15 s to accelerate the desorption process. The analyte-rich phase was transferred to a clean centrifuge tube and was sent to the FAAS system.

Preparation of synthetic and real domestic wastewater

The domestic wastewater was obtained from the advanced biological treatment wastewater plant in İstanbul. As domestic wastewater was not obtained from a different location, a second matrix was synthetically prepared in the laboratory for use in the matrix-matching strategy. Accordingly, synthetic domestic wastewater was prepared by slightly modifying the synthetic domestic wastewater procedure given in the literature (Turan et al. 2020). In this procedure, 0.0422 g $MgSO_4$, 0.1058 g $(NH_4)_2SO_4$, 0.0020 g $MnSO_4$, 0.063 g $CaCl_2$, 0.0249 g KH_2PO_4, 0.0114 g $FeCl_3$, 0.2573 g $NaHCO_3$, 0.1157 g bactopeptone, 0.0149 g yeast extract, and 0.4403 g glucose were weighed and dissolved in 1.0 L tap water.

Silver ions can form stable complexes with bromo, chloro, and iodo ligands in the sample matrix, which can affect the accuracy of the recovery results. Therefore, a procedure was applied to remove anions from the environment before applying the extraction method to the samples (Soylak et al. 2000). The suspended solids in wastewater were precipitated by centrifugation. 10.0 mL of the supernatant was taken and filtered through grade 1 Whatman filter paper (11 µm) filled with 250 mg resin. After filtration, 5.0 mL of the solution was diluted to 250 mL. The water used in this dilution process was also passed through the resin. These steps were performed separately for two different matrices. To ensure that the conditions were the same for external calibration standards, the deionized water used in standard preparation was passed through the resin similarly. This avoids the AgCl precipitation problem caused by chlorine ions. Moreover, the applicability of the method in real sample matrices is increased. For the recovery study, care was taken to keep the sample solution grams constant during spiking and samples were prepared gravimetrically.

Results and discussion

Characterization studies

A characterization study was carried out to determine and compare the morphological and structural properties of TiO_2 NPs and $TiO_2@Fe_3O_4$ NCs synthesized under different conditions. The influence of temperature and precursor solution on morphology and size distribution was investigated to determine the optimum TiO_2 NPs procedure for the synthesis of $TiO_2@Fe_3O_4$ NCs.

It was predicted that the morphology of TiO_2 could be changed by modifying the HCl/H_2O and $TTIP/H_2O$ ratios in the precursor solution. This can be attributed to TiO_2 synthesis beginning with a hydrolysis reaction, and H_2O content is pivotal in this step (Haidry et al. 2024). The –OH group in H_2O is substituted by the –OR group in TTIP (Cargnello et al. 2014). When the H_2O content in the solution is insufficient, the hydrolysis rate decreases, or it becomes difficult for the alcoholates to dissolve completely in the medium (Gatou et al. 2024). On the other hand, the acid catalyst can affect the structure of the condensed product. Furthermore, it can affect the rate of condensation and hydrolysis steps (Cihlar et al. 2013). Therefore, the effect of $TTIP/H_2O$ and HCl/H_2O ratios on the structure was investigated. SEM images of TiO_2 particles prepared with precursor solution-A and solution-B using the temperature program-1 given in Table 1 are compared in Fig. 1. It was clearly seen that the variations in the precursor solution affected the structure. A more homogeneous size distribution was observed when precursor solution-A was used.

The effect of temperature, another parameter expected to affect the structure, is examined in the next step. For this purpose, zeta potential measurements of TiO_2 NPs synthesized by following three different temperature programs in Table 1 were taken. As a result, it was seen that the particle size distribution was mostly in the range of 100–1000 nm in program-1 at 145 °C. At 150 °C and 155 °C, it was determined that the particle size distribution was more intense in the range of 10–100 nm. Figure 2 shows the particle size density distribution graph of TiO_2 NPs prepared with program-3.

The FE-SEM recorded images of TiO_2 NPs, Fe_3O_4 NPs and $TiO_2@Fe_3O_4$ NPs to show that TiO_2 colloidal nanoparticles were coated on the Fe_3O_4 surface. The

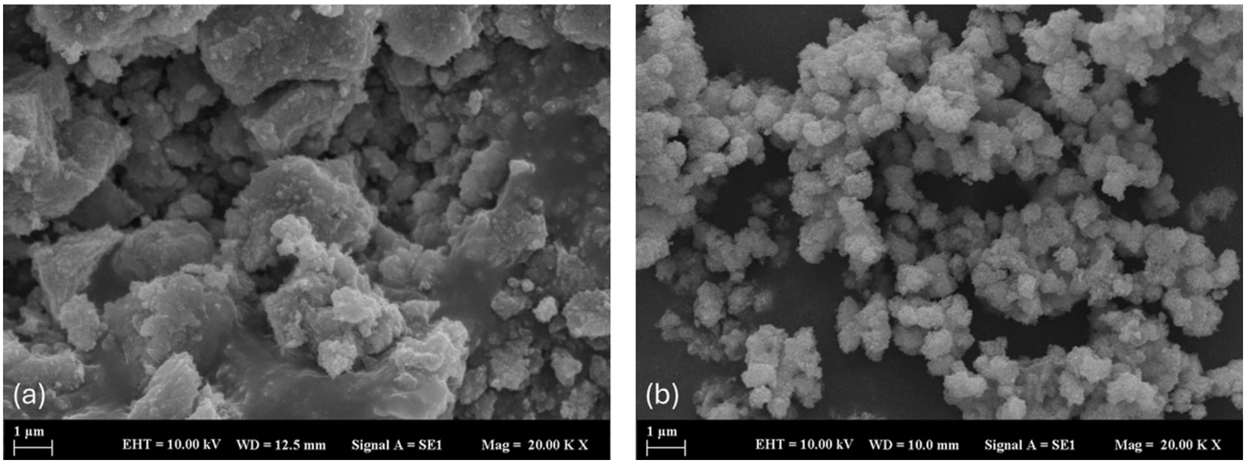

Fig. 1 SEM images of TiO_2 structures were acquired through program-1, and these were magnified 20,000 times: Image of **a** was prepared with precursor solution-B, and image of **b** was prepared with precursor solution-A

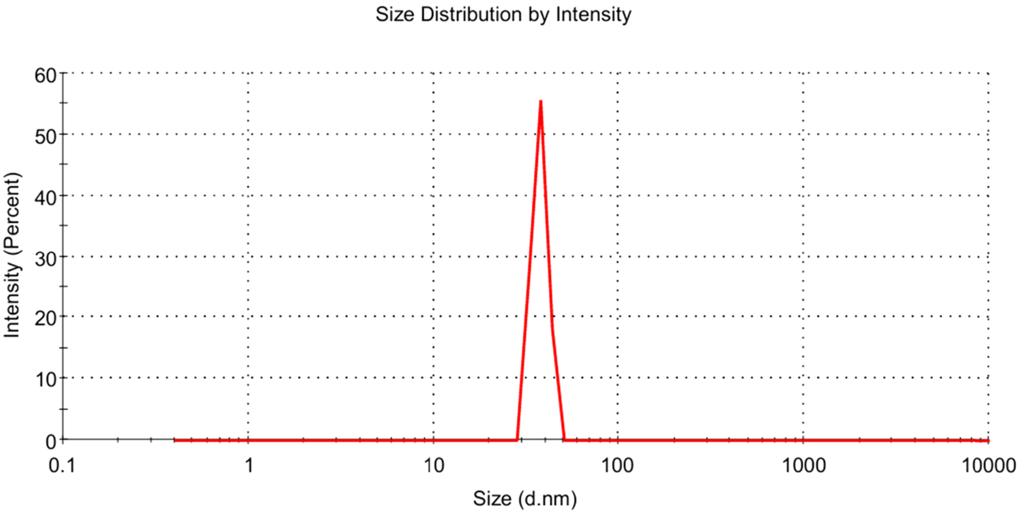

Fig. 2 The particle size distribution of TiO_2 nanoparticles was prepared under conditions where A-precursor solution was used, and the final temperature was elevated to 155 °C

micrograph given in Fig. 3a belongs to TiO_2 NPs. Figure 3b shows the porous structure of Fe_3O_4 NPs. In the $TiO_2@Fe_3O_4$ NPs presented in Fig. 3c, it is seen that the porosity decreases due to the coating of Fe_3O_4 NPs with TiO_2NPs.

XRD diffractograms of TiO_2, Fe_3O_4, and $TiO_2@Fe_3O_4$ nanostructures are examined in Fig. 3d, e and f and compared with the literature. The position of the diffraction peaks at 2θ of TiO_2 NPs was found at 25.36°, 37.51°, 48.06°, 54.21°, 54.56°, 62.68°, 69.87°, 75.07°, and 82.35°. These positions were confirmed as belonging to the TiO_2 structure by comparison with the ICSD Ref. # 00-021-1272 card and other anatase phase TiO_2 structures in the literature (Akram et al. 2021; Lü et al. 2019). Diffraction peak positions for Fe_3O_4 NPs were obtained at 30.36°, 35.62°, 43.38°, 53.74°, 57.23°, and 62.83°. These values were determined to be consistent with the characteristic diffraction peak positions in JCPDS card 19–0629, and it was concluded that the structure is in cubic phase (Alfredo Reyes Villegas et al. 2020; Khashan et al. 2017; Wu et al. 2020; Yan et al. 2016). When the XRD pattern of $TiO_2@Fe_3O_4$ NCs was examined, the elevated difference in counts from TiO_2 and Fe_3O_4 structures caused the nanocomposite pattern to appear more like the Fe_3O_4 nanoparticle structure. However, comparing the patterns of the $TiO_2@Fe_3O_4$ NCs structure in the literature and

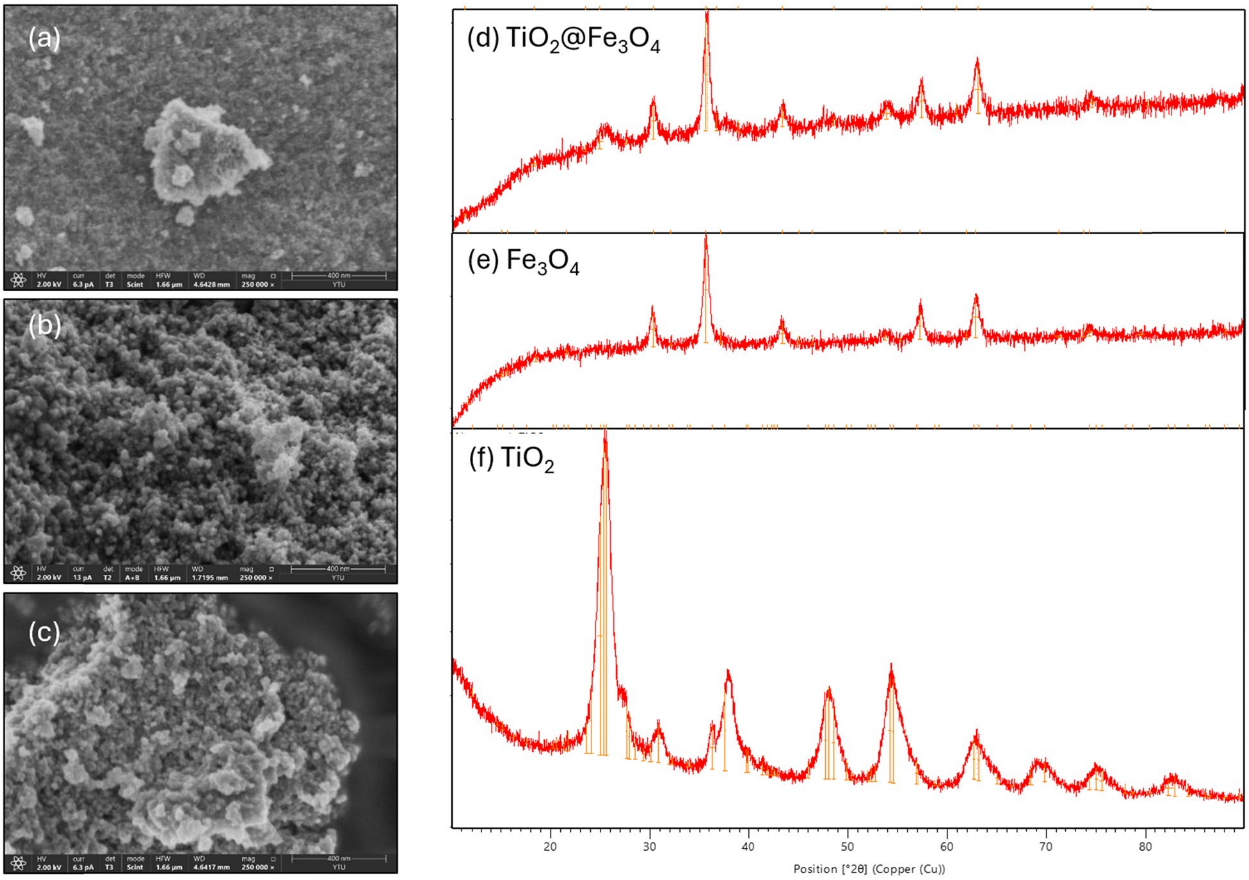

Fig. 3 FE-SEM micrographs for **a** TiO_2; **b** Fe_3O_4; **c** $TiO_2@Fe_3O_4$ nanomaterials and XRD patterns for **d** TiO_2; **e** Fe_3O_4; **f** $TiO_2@Fe_3O_4$

the synthesized $TiO_2@Fe_3O_4$ NCs structure, it is concluded that the patterns are remarkably similar to each other. In both patterns, a formation of a new diffraction peak at the 20–25° positions, which was not observed in Fe_3O_4 structure, was observed (Yan et al. 2016). This demonstrated that $TiO_2@Fe_3O_4$ NCs were successfully synthesized.

Optimization studies

Optimization buffer solution conditions

When the pH and ionic strength of the solution medium change, the surface charge of the analyte and sorbent can alter; as a result, electrostatic attraction or repulsion can be observed between the analyte and the sorbent. This is a significant factor that can improve the extraction efficiency (Ghorbani et al. 2020). In order to investigate the effect of pH on extraction efficiency, buffer solutions adjusted to different pH values were prepared and added to aqueous standard solutions. Simultaneously, experiments were performed without buffer addition. In the absence of a buffer in the aqueous solution, adsorption occurred, but the extraction outputs were not repeatable. In alkaline medium (pH 8.0–9.0), the low interaction between the analyte and the nanoparticle is clearly seen in Fig. 4a. No analytical signal was obtained when tris–HCl buffer solution (pH 7.0) was used. This can be attributed to the complexation of tris with silver (Babel et al. 2020). The highest average absorbance value in acidic medium was obtained in potassium hydrogen phthalate-NaOH (pH 6.0) buffer solution. Therefore, potassium hydrogen phthalate-NaOH (pH 6.0) buffer solution was selected as the optimum condition and the volume of buffer solution used was tested in the range of 0.5–2.0 mL. The highest extraction yield was obtained at 1.5 mL which was determined as the optimum volume.

Optimization of agitation conditions

The applicability and scalability of the methods developed in recent years have been as relevant as their greenness. It is desirable to reduce the need for human intervention and increase the number of samples that can be processed simultaneously (Manousi et al. 2023). In order to increase the applicability of the developed method, instead of vortexing, orbital shaking and

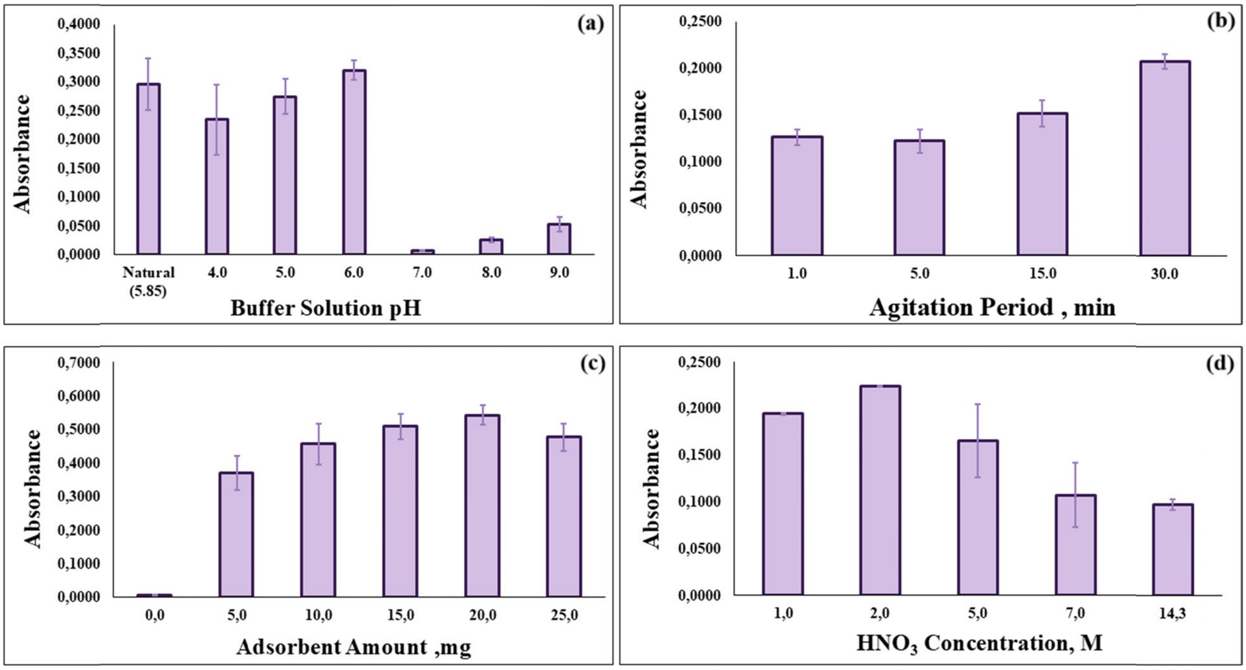

Fig. 4 Effect of **a** buffer solution pH, **b** agitation period, **c** adsorbent amount, and **d** desorption solvent concentration on the separation/preconcentration performance of silver ions

ultrasonic mixing methods that provide such possibilities were investigated. Ultrasonication resulted in the dissolution of the nanoparticles. Therefore, it was decided to continue experimental studies with the orbital agitation method without analytical comparison. Afterward, the effect of the contact time between $TiO_2@Fe_3O_4$ NCs and silver ions on the extraction efficiency was investigated in the range of 1.0–30.0 min using an orbital shaker. As seen in Fig. 4b, there is no significant difference between the mean absorbance values at 1.0 min and 5.0 min. Extraction efficiency was enhanced by increasing contact time over 5 min. Agitation periods over 30.0 min were not evaluated, as prolonged agitation would result in an excessively protracted sample preparation procedure, hence dramatically diminishing the number of samples that can be processed within an hour. The experiments were continued with a mixing duration of 30.0 min.

Optimization of adsorbent amount

The increasing amount of adsorbent leads to an increase in adsorption sites, and accordingly, an improvement in adsorption capacity is expected to be observed. However, when the amount of adsorbent is more than necessary, it may cause a decrease in the surface area of the adsorbent by means of agglomeration. In addition, the excessive bulk of material can lead to difficulties in desorption, leading to a decrease in adsorption capacity. Hence, the quantity of adsorbent is a highly crucial parameter to be determined in the extraction procedure (Wadhawan et al. 2020). Accordingly, the effect of nanoparticle amount on adsorption capacity was tested in the dosage range of 0.0–25.0 mg. The results supported the hypothesis as shown in Fig. 4c. It was seen that the adsorption capacity increases with the increment in the amount of adsorbent up to 20.0 mg. A decrease in adsorption capacity was observed above 20.0 mg. Simultaneously, the same experimental procedure was performed without the nanoparticles, but no analytical signal was observed. This indicated that the extraction procedure was based on sorption and not on precipitation of silver species. 20.0 mg of ideal adsorbent amount was selected, and optimization studies were continued.

Optimization of desorption conditions

The concentration and volume of the eluent HNO_3 solution were studied to ensure that all analytes on the adsorbent were desorbed and to maximize the concentration of analytes to be atomized. Initially, the concentration of the HNO_3 solution was tested in the concentration range of 1.0–14.3 M as shown in Fig. 4d. The higher viscosity at the high concentration reduced the rate at which analytes were transported to the flame. As this reduces the degree of atomization, a decrease in the mean absorbance values was seen with increasing concentration above 2.0 M. On the other side, a notable decrease in absorbance was observed below 2.0 M, indicating an insufficient desorption of analytes from the nanocomposite. Therefore, the ideal concentration of the HNO_3 solution was chosen at 2.0 M. The volume of the desorption solution was then tested in the range of 75–200 µL. The mean absorbance values obtained at 75 µL and 100 µL were very close. However, the signals in 75 µL did not have the necessary saturation for quantitative determination. Hence, the experimental studies were continued with 100 µL.

The analytical performance of the TiO_2@Fe_3O_4-MDSPE-FAAS system

In order to evaluate the analytical performance of FAAS and MDSPE-FAAS systems for the determination of silver ions, standard aqueous solutions were prepared at increasing concentrations. All standards and samples in this study were prepared gravimetrically by the help of a sensitive balance. The optimum conditions of the MDSPE method determined as a result of the optimization studies are summarized in Table 2 and applied to the standard aqueous solutions prepared for the MDSPE-FAAS system.

The limit of detection (LOD), limit of quantification (LOQ), the enhancement in calibration sensitivity (ECS), and the enhancement in detection power (EDP) were calculated by using the calibration lines achieved. The equations utilized in the calculations are given below:

$$\mathrm{LOD} = s_{\mathrm{LC}}/m \times 3 \tag{1}$$

$$\mathrm{LOD} = s_{\mathrm{LC}}/m \times 10 \tag{2}$$

$$\mathrm{ECS} = m_1/m_2 \tag{3}$$

$$\mathrm{ECS} = \mathrm{LOD}_1/\mathrm{LOD}_2 \tag{4}$$

In the equations, s_{LC} represents the standard deviation of the signal obtained for the lowest concentration; m represents the slope of the line; m_1 and m_2 represent the slopes of the calibration lines obtained from MDSPE-FAAS and FAAS systems, respectively; LOD_1 and LOD_2 represent the LOD values calculated for FAAS and MDSPE-FAAS systems, respectively.

The coefficient of determination (R^2) values of the developed MDSPE-FAAS and FAAS systems are above 0.999. LOD-LOQ values were calculated to be 0.005–0.017 mg kg^{-1} for MDSPE-FAAS and 0.069–0.229 mg kg^{-1} for FAAS, respectively. The new approach shows an enhancement in both sensitivity and detection limit for analyte determination. The regression equations for the calibration lines for the FAAS and the MDSPE-FAAS systems were defined as $y = 0.0601x + 0.0056$and $y = 1.5815x + 0.0101$, respectively. The ECS value, which is a measure of these improvements, was calculated as 26.31 and the EDP value as 13.42. In Table 3, the analytical performance values of the developed method are compared with different studies in the literature. The results revealed that TiO_2@Fe_3O_4 NCs-based MDSPE method can be used as an alternative method for determination of Ag ions at trace levels.

Table 2 Optimum conditions of the MDSPE method developed for the determination of silver ions

Parameter	Conditions
Sample volume	8.0 mL
Buffer solution type/volume	pH 6/1.5 mL
Amount of TiO_2@Fe_3O_4 NCs	20.0 mg
Agitation type/period	Orbital Shaker/30.0 min
HNO_3 solution concentration/volume	2.0 M/ 0.10 mL

Recovery studies

In complex matrices such as wastewaters, there might be many inorganic and organic components which have the potential to interfere with TiO_2@Fe_3O_4 NCs or Ag ions. These components may affect the results of the analysis, so the applicability of the method was investigated by conducting a spike-recovery study. For this purpose, calibration lines were established in the concentration ranges of 0.080–0.150 mg kg^{-1} for synthetic domestic wastewater samples, 0.020–0.080 mg kg^{-1} for real domestic wastewater, and 0.020–0.157 mg kg^{-1} for deionized water samples. The percentage recovery results of the spiked

Table 3 Comparison of various system performance values of the developed method with the literature

Method	Sample Volume	LOD, mg L^{-1}	LOQ, mg L^{-1}	Linear Range, mg L-1	Ref
EA-DLLME-FA-MS-FAAS	10.0 mL	0.002	0.003	0.005–0.150	Ghoochani Moghadam et al., (2017)
UA-EME-FAAS	5.0 mL	0.0068	0.023	0.055–1.5	Khayatian and Pourbahram, (2016)
SPE-FAAS	100 mL	0.04	0.133	–	Refiker et al., (2008)
CPE-FAAS	14.0 mL	0.010	–	0.028–0.430	Tavallali et al., (2010)
FAAS	–	0.069 (mg kg^{-1})	0.229 (mg kg^{-1})	0.10–10.27 (mg kg^{-1})	This Study
MDSPE-FAAS	8.0 mL	0.005 (mg kg^{-1})	0.017 (mg kg^{-1})	0.010–0.301(mg kg^{-1})	This Study

synthetic and real domestic wastewater samples were calculated by external calibration method using the calibration line prepared with deionized water. It was observed that the calculated results were not within acceptable limits. Therefore matrix-matching calibration strategy was used to eliminate interference effects. In this strategy, the percentage recovery values of the real domestic wastewater sample spiked at 0.080 mg kg^{-1} were calculated using the calibration plotted for the synthetic domestic wastewater. Similarly, the percentage recovery values of synthetic domestic wastewater samples spiked at 0.080 mg kg^{-1} were calculated based on the calibration established with real domestic wastewater. The percentage recovery results are summarized in Table 4.

Conclusion

TiO_2 NPs and $TiO_2@Fe_3O_4$ NCs were synthesized with an innovative approach, and the nanomaterials were characterized by using SEM, FE-SEM, and XRD methods. Characterization studies demonstrated that the particle size of the prepared TiO_2 NPs was at the nanoscale and the surface of the Fe_3O_4 NPs was modified with the TiO_2 NPs in the obtained nanocomposite. A novel MDSPE method for the determination of Ag ions was developed by using $TiO_2@Fe_3O_4$ NCs. The developed method enables the determination of Ag at trace levels, and the $TiO_2@Fe_3O_4$-MDSPE-FAAS technique was found to be highly effective when compared with alternative methods in the literature. The LOD and LOQ values of the developed method are 0.005 mg kg^{-1} and 0.017 mg kg^{-1}, respectively. The linear range is between 0.010 and 0.301 mg kg^{-1}. These values are promising as they allow for determination well below the maximum limits recommended by EPA and WHO. Moreover, the developed system offers 26.31 times better calibration sensitivity and 13.42 times better detection power than the FAAS system alone. The results of recovery studies on real and synthetic wastewater samples showed that the developed method has the potential to be implemented in the analysis of complex matrices. However, the recovery study showed that the recovery results are not within the acceptable range when external calibration is used. Therefore, following the matrix-matching strategy when using the $TiO_2@Fe_3O_4$-MDSPE-FAAS technique, especially in complex matrices, has been a highlight of the developed method. Moreover, $TiO_2@Fe_3O_4$ NCs have not been previously reported for the preconcentration and separation of any heavy metals from domestic wastewater samples. This contributes to the novelty of this study and paves the way for the development of $TiO_2@Fe_3O_4$-MDSPE-FAAS techniques for the determination of different heavy metals in domestic wastewater.

Table 4 Calculation of the percentage recovery values of Ag ions spiked in different wastewater matrices by matrix-matching method

Domestic wastewater type	Spiked Ag concentration, mg kg^{-1}	Calculated Silver concentration, mg kg^{-1}	%Recovery ± SD
Real	0.080	0.071	89.49 ± 3.44
Synthetic	0.080	0.083	103.68 ± 3.62

Acknowledgements

The authors would like to thank the 'Scientific and Technological Research Council of Turkey' for financial support.

Author contributions

Hilal Akbıyık helped in writing—original draft, visualization, validation, methodology, investigation, formal analysis, data curation. Ayça Girgin was involved in writing—original draft, visualization, validation, methodology, investigation, formal analysis, data curation. Buse Tuğba Zaman contributed to writing—original draft, visualization, validation, methodology, investigation, formal analysis, data curation. Arda Atakol helped in writing—original draft, visualization, validation, methodology, investigation, data curation. Nevim San contributed to validation, methodology, investigation. Sezgin Bakırdere helped in writing—review & editing, supervision, conceptualization, methodology, investigation, data curation.

Funding

This study was supported by TÜBİTAK-BİDEB-2209 within the scope of university students research projects support program with funding number 1919B012205925.

Availability of data and materials

Data will be made available on request.

Declarations

Ethics approval and consent to participate

Not applicable.

Consent to publish

I hereby provide consent for the publication of the manuscript.

Competing interests

The authors declare that they have no known competing financial interests or personal relationships that could have appeared to influence the work reported in this paper.

Author details

[1]Chemistry Department, Yıldız Technical University, 34220 Istanbul, Türkiye. [2]Neutec Pharmaceutical, Yıldız Technical University Teknopark, 34220 Istanbul, Türkiye. [3]Faculty of Pharmacy, İstinye University, 34010 Istanbul, Türkiye. [4]Scientific and Technological Research Application and Research Center, İstinye University, 34010 Istanbul, Türkiye. [5]Faculty of Pharmacy, İstanbul Kent University, 34406 Istanbul, Türkiye. [6]Turkish Academy of Sciences (TÜBA), Vedat Dalokay Street, No: 112, Çankaya, 06670 Ankara, Türkiye.

Received: 18 March 2025 Accepted: 2 June 2025

References

Ahmadi M, Elmongy H, Madrakian T, Abdel-Rehim M. Nanomaterials as sorbents for sample preparation in bioanalysis: a review. Anal Chim Acta. 2017;958:1–21. https://doi.org/10.1016/J.ACA.2016.11.062.

Akram M, Khan RM, Afzal F, Mustafa GM, Ahmad A, Ramay SM, Mahmood A, Ali SM, Atiq S. CNTs mediated electrochemical performance and dielectric dispersion of TiO_2-based hydrothermally synthesized nanocomposites. Ionics (Kiel). 2021;27:2107–18. https://doi.org/10.1007/S11581-021-03953-X/FIGURES/10.

Aladaghlo Z, Malekzadeh S, Sahragard A, Fakhari AR. Synthesis of Fe_3O_4@SiO_2-creatine as a new nanosorbent for dispersive magnetic solid-phase microextraction of copper ions from water, food, and soil samples. J Food Compos Anal. 2024;129: 106097. https://doi.org/10.1016/J.JFCA.2024.106097.

Al-Saidi HM, Khan S. A review on organic fluorimetric and colorimetric chemosensors for the detection of Ag(I) ions. Crit Rev Anal Chem. 2024;54:1810–36. https://doi.org/10.1080/10408347.2022.2133561.

Al-Salihi S, Bayati M, Jasim AM, Fidalgo MM, Xing Y. Magnetic mesoporous TiO_2/Fe_3O_4 nanocomposite adsorbent for removal of sulfamethazine from water. Environ Adv. 2022;9: 100283. https://doi.org/10.1016/J.ENVADV.2022.100283.

Babel L, Bonnet-Gómez S, Fromm KM. Appropriate buffers for studying the bioinorganic chemistry of silver(I). Chemistry. 2020;2:193–202. https://doi.org/10.3390/CHEMISTRY2010012.

Cargnello M, Gordon TR, Murray CB. Solution-phase synthesis of titanium dioxide nanoparticles and nanocrystals. Chem Rev. 2014;114:9319–45. https://doi.org/10.1021/CR500170P/ASSET/CR500170P.FP.PNG_V03.

Choi C, Cui Y. Recovery of silver from wastewater coupled with power generation using a microbial fuel cell. Bioresour Technol. 2012;107:522–5. https://doi.org/10.1016/J.BIORTECH.2011.12.058.

Chronakis MI, Mavrakis E, García RÁF, Montes-Bayón M, Bettmer J, Pitta P, Tsapakis M, Kalantzi I, Tsiola A, Pergantis SA. Investigating the behavior of ultratrace levels of nanoparticulate and ionic silver in a seawater mesocosm using single particle inductively coupled plasma – mass spectrometry. Chemosphere. 2023;336: 139109. https://doi.org/10.1016/J.CHEMOSPHERE.2023.139109.

Cihlar J, Cihlar J, Bartonickova E. Low-temperature sol-gel synthesis of anatase nanoparticles modified by Au, Pd and Pt and activity of TiO_2/Au, Pd, Pt photocatalysts in water splitting. J Sol-Gel Sci Technol. 2013;65:430–42. https://doi.org/10.1007/S10971-012-2955-8/TABLES/5.

El Hafidi EM, Mortadi A, Chahid EG, Laasri S. Monitoring of domestic wastewater treatment via infiltration percolation using impedance spectroscopy. Environ Technol Innov. 2023;32: 103421. https://doi.org/10.1016/J.ETI.2023.103421.

Gao Z, Liu GG, Ye H, Rauschendorfer R, Tang D, Xia X. Facile colorimetric detection of silver ions with picomolar sensitivity. Anal Chem. 2017;89:3622–9. https://doi.org/10.1021/acs.analchem.6b05026.

Gasbarri C, Ruggieri F, Foschi M, Aceto A, Scotti L, Angelini G. Simple determination of silver nanoparticles concentration as Ag+ by using ISE as potential alternative to ICP optical emission spectrometry. ChemistrySelect. 2019;4:9501–4. https://doi.org/10.1002/SLCT.201902336.

Gatou MA, Syrrakou A, Lagopati N, Pavlatou EA. Photocatalytic TiO_2-based nanostructures as a promising material for diverse environmental applications: a review. Reactions. 2024;5:135–94. https://doi.org/10.3390/REACTIONS5010007.

Ghoochani Moghadam A, Rajabi M, Hemmati M, Asghari A. Development of effervescence-assisted liquid phase microextraction based on fatty acid for determination of silver and cobalt ions using micro-sampling flame atomic absorption spectrometry. J Mol Liq. 2017;242:1176–83. https://doi.org/10.1016/J.MOLLIQ.2017.07.038.

Ghorbani M, Aghamohammadhassan M, Ghorbani H, Zabihi A. Trends in sorbent development for dispersive micro-solid phase extraction. Microchem J. 2020;158: 105250. https://doi.org/10.1016/J.MICROC.2020.105250.

Gutiérrez-Fernández L, San Andrés MP, Díez-Pascual AM. Nanomaterials as sorbents in solid-phase extraction for bioactive compounds. Sep Purif Rev. 2024. https://doi.org/10.1080/15422119.2024.2362401.

Habila MA, Alothman ZA, El-Toni AM, Labis JP, Soylak M. Synthesis and application of Fe_3O_4@SiO_2@TiO_2 for photocatalytic decomposition of organic matrix simultaneously with magnetic solid phase extraction of heavy metals prior to ICP-MS analysis. Talanta. 2016;154:539–47. https://doi.org/10.1016/J.TALANTA.2016.03.081.

Haidry AA, Yucheng W, Fatima Q, Raza A, Zhong L, Chen H, Mandebvu CR, Ghani F. Synthesis and characterization of TiO_2 nanomaterials for sensing environmental volatile compounds (VOCs): a review. TrAC Trends Anal Chem. 2024;170: 117454. https://doi.org/10.1016/J.TRAC.2023.117454.

Huang W, Liang Y, Deng Y, Cai Y, He Y. Prussian blue nanoparticles as optical probes for visual and spectrophotometric determination of silver ions. Microchim Acta. 2017;184:2959–64. https://doi.org/10.1007/S00604-017-2328-7/TABLES/2.

Jagirani MS, Soylak M. A review: recent advances in solid phase microextraction of toxic pollutants using nanotechnology scenario. Microchem J. 2020;159: 105436. https://doi.org/10.1016/J.MICROC.2020.105436.

Ji Z, Shu Y, Xu Q, Hu X. Ultrasensitive electrochemiluminescence determination of trace Ag ions based on the signal amplification caused by its catalytic effect on Mn(II) oxidation using graphite catheter as electrode. Talanta. 2018;187:188–92. https://doi.org/10.1016/J.TALANTA.2018.05.029.

Kaur M, Virender, Khatkar S, Singh B, Kumar A, Dubey SK. Recent advancements in sensing of silver ions by different host molecules: an overview (2018–2023). J Fluoresc. 2023. https://doi.org/10.1007/S10895-023-03494-8.

Khashan S, Dagher S, Tit N, Alazzam A, Obaidat I. Novel method for synthesis of Fe_3O_4@TiO_2 core/shell nanoparticles. Surf Coatings Technol. 2017;322:92–8. https://doi.org/10.1016/J.SURFCOAT.2017.05.045.

Khayatian G, Pourbahram B. Ultrasound-assisted emulsification microextraction and preconcentration of trace amounts of silver ions as a cyclam complex. J Anal Sci Technol. 2016;7:1–8. https://doi.org/10.1186/S40543-016-0083-8/TABLES/3.

Khezeli T, Daneshfar A. Development of dispersive micro-solid phase extraction based on micro and nano sorbents. TrAC Trends Anal Chem. 2017;89:99–118. https://doi.org/10.1016/J.TRAC.2017.01.004.

Liu T, Fu L, Yin C, Wu M, Chen L, Niu N. Design of smartphone platform by ratiometric fluorescent for visual detection of silver ions. Microchem J. 2022;174: 107016. https://doi.org/10.1016/J.MICROC.2021.107016.

Liu Z, Qi P, Zhao H, Wang J, Wang Z, Di S, Xu H, Wang Q, Wang X. Fabrication and application of hydrangea-like magnetic titanium dioxide (Fe_3O_4–TiO_2) particles: development of magnetic "one-step" pretreatment method for multi-pesticide residues analysis in fish. Environ Pollut. 2023;327: 121574. https://doi.org/10.1016/J.ENVPOL.2023.121574.

Lü X, Hao P, Xie G, Duan J, Gao L, Liu B. A sensor array realized by a single flexible TiO_2/POMs film to contactless detection of triacetone triperoxide. Sensors. 2019;19:915. https://doi.org/10.3390/S19040915.

Manousi N, Wojnowski W, Płotka-Wasylka J, Samanidou V. Blue applicability grade index (BAGI) and software: a new tool for the evaluation of method practicality. Green Chem. 2023;25:7598–604. https://doi.org/10.1039/D3GC02347H.

Muoghalu CC, Owusu PA, Lebu S, Nakagiri A, Semiyaga S, Iorhemen OT, Manga M. Biochar as a novel technology for treatment of onsite domestic wastewater: a critical review. Front Environ Sci. 2023;11:1095920. https://doi.org/10.3389/FENVS.2023.1095920/BIBTEX.

Naeemullah, Kazi TG, Afridi HI, Shah F, Arain SS, Brahman KD, Ali J, Arain MS. Simultaneous determination of silver and other heavy metals in aquatic environment receiving wastewater from industrial area, applying an enrichment method. Arab J Chem. 2016;9:105–13. https://doi.org/10.1016/J.ARABJC.2014.10.027.

Nguyen DV, Wu D. Recent advances in innovative osmotic membranes for resource enrichment and energy production in wastewater treatment. Sci Total Environ. 2024;927: 172153. https://doi.org/10.1016/J.SCITOTENV.2024.172153.

Ouyang J, Zhan L, Luo Q, Miao J, Hu L, He X, Wang X. Adsorption performance of silver ion on acrylic grafted carboxymethyl chitosan/dialdehyde starch. Adsorption. 2024;30:1225–37. https://doi.org/10.1007/S10450-024-00501-7/FIGURES/12.

Płotka-Wasylka J, Szczepańska N, de la Guardia M, Namieśnik J. Miniaturized solid-phase extraction techniques. TrAC Trends Anal Chem. 2015;73:19–38. https://doi.org/10.1016/J.TRAC.2015.04.026.

Pyrzynska K. Nanomaterials in speciation analysis of metals and metalloids. Talanta. 2020;212: 120784. https://doi.org/10.1016/J.TALANTA.2020.120784.

Refiker H, Merdivan M, Aygün RS. Solid-phase extraction of silver in geological samples and its determination by FAAS. Sep Sci Technol. 2008;43:179–91. https://doi.org/10.1080/01496390701764833.

Roushani M, Baghelani YM, Abbasi S, Mohammadi SZ, Zahedifar M, Mavaei M. Separation of Ag(I) ions from *Lepidium draba* L. plant and water and standard samples by carrier element-free coprecipitation method prior to their flame atomic absorption spectrometric determination. Commun Soil Sci Plant Anal. 2016;47:1207–15. https://doi.org/10.1080/00103624.2016.1166381.

Sajid M, Płotka-Wasylka J. Combined extraction and microextraction techniques: recent trends and future perspectives. TrAC Trends Anal Chem. 2018;103:74–86. https://doi.org/10.1016/J.TRAC.2018.03.013.

Seetasang S, Iwai CB. Enhancing domestic wastewater treatment: Integrating vermifiltration and biochar for heavy metal and microplastic reduction and by-product utilization. Case Stud Chem Environ Eng. 2025;11: 101025. https://doi.org/10.1016/J.CSCEE.2024.101025.

Song X, Gunawan P, Jiang R, Leong SSJ, Wang K, Xu R. Surface activated carbon nanospheres for fast adsorption of silver ions from aqueous solutions. J Hazard Mater. 2011;194:162–8. https://doi.org/10.1016/J.JHAZMAT.2011.07.076.

Soylak M, Elci L, Dogan M. A sorbent extraction procedure for the preconcentration of gold, silver and palladium on an activated carbon column. Anal Lett. 2000;33:513–25. https://doi.org/10.1080/00032710008543070.

Spietelun A, Kloskowski A, Chrzanowski W, Namieśnik J. Understanding solid-phase microextraction: key factors influencing the extraction process and trends in improving the technique. Chem Rev. 2013;113:1667–85. https://doi.org/10.1021/CR300148J/ASSET/IMAGES/MEDIUM/CR-2012-00148J_0005.GIF.

Tang L, Lan G, Ma P, Jia Y, Zhang X, Luo P, Wei W. Ultrasensitive detection of trace silver ions using MoS42−-intercalated LDH nanosheets enhanced SPR sensor. Sensors. 2024;24:5973. https://doi.org/10.3390/S24185973.

Tavallali H, Yazdandoust S, Yazdandoust M. Cloud point extraction for the preconcentration of silver and palladium in real samples and determination by atomic absorption spectrometry. CLEAN Soil Air Water. 2010;38:242–7. https://doi.org/10.1002/CLEN.200900207.

Turan NB, Erkan HS, Chormey DS, Cağlak A, Bakirdere S, Engin GO. Feasibility studies on the effect of natural plant compounds on sludge characteristics in a batch-type aerobic reactor and N-butyryl-L homoserine lactone. Anal Lett. 2020;53:2431–44. https://doi.org/10.1080/00032719.2020.1745222.

van den Brand TPH, Roest K, Chen GH, Brdjanovic D, van Loosdrecht MCM. Potential for beneficial application of sulfate reducing bacteria in sulfate containing domestic wastewater treatment. World J Microbiol Biotechnol. 2015;31:1675–81. https://doi.org/10.1007/S11274-015-1935-X/FIGURES/1.

Villegas VAR, Ramírez JIDL, Guevara EH, Sicairos SP, Ayala AHL, Landeros LB. Synthesis and characterization of magnetite nanoparticles for photocatalysis of nitrobenzene. J Saudi Chem Soc. 2020;24:223–35. https://doi.org/10.1016/J.JSCS.2019.12.004.

Wadhawan S, Jain A, Nayyar J, Mehta SK. Role of nanomaterials as adsorbents in heavy metal ion removal from waste water: a review. J Water Process Eng. 2020;33: 101038. https://doi.org/10.1016/J.JWPE.2019.101038.

Wu H, Hao L, Chen C, Zhou J. Superhydrophobic Fe$_3$O$_4$/OA magnetorheological fluid for removing oil slick from water surfaces effectively and quickly. ACS Omega. 2020;5:27425–32. https://doi.org/10.1021/ACSOMEGA.0C03857/ASSET/IMAGES/MEDIUM/AO0C03857_M003.GIF.

Wu S, Han C, Fu W, Gong X, Jiang Z, Wang Y, Zhang P. Smartphone-enabled colorimetric determination of silver ions exploiting the peroxidase-mimetic behavior of bowl-shaped Pd3Pt nanocrystals. Microchem J. 2023;195: 109434. https://doi.org/10.1016/J.MICROC.2023.109434.

Xia L, Yang J, Su R, Zhou W, Zhang Y, Zhong Y, Huang S, Chen Y, Li G. Recent progress in fast sample preparation techniques. Anal Chem. 2020;92:34–48. https://doi.org/10.1021/ACS.ANALCHEM.9B04735/ASSET/IMAGES/LARGE/AC9B04735_0005.JPEG.

Xu L, Wang YY, Huang J, Chen CY, Wang ZX, Xie H. Silver nanoparticles: synthesis, medical applications and biosafety. Theranostics. 2020;10:8996–9031. https://doi.org/10.7150/THNO.45413.

Yalcin M. The effect of pH on the physical and structural properties of TiO$_2$ nanoparticles. J Cryst Growth. 2022;585: 126603. https://doi.org/10.1016/J.JCRYSGRO.2022.126603.

Yan L, Wang Y, Li J, Shen H, Wang C, Yang S. A facile approach for the synthesis of sea urchin-like Fe$_3$O$_4$@TiO$_2$@Ag nanocomposites as highly efficient and recyclable photocatalysts. J Mater Sci Mater Electron. 2016;27:10616–21. https://doi.org/10.1007/S10854-016-5156-3/FIGURES/9.

Zengin HB, Gürkan R. Eco-friendly trace analysis of silver in beer/wine samples using a new co-polymeric nanocomposite based-ultrasound assisted-cloud point extraction combined with spectrophotometry. J Food Compos Anal. 2021;98: 103814. https://doi.org/10.1016/J.JFCA.2021.103814.

Publisher's Note